



## Full Length Article

# Parametrizing nonbonded interactions between silica and water from first principles



H. Gokberk Ozcelik<sup>a</sup>, Yigit Sozen<sup>b</sup>, Hasan Sahin<sup>b</sup>, Murat Barisik<sup>a,\*</sup>

<sup>a</sup> Department of Mechanical Engineering, Izmir Institute of Technology, IZMIR, 35430, Turkey

<sup>b</sup> Department of Photonics, Izmir Institute of Technology, IZMIR, 35430, Turkey

## ARTICLE INFO

## Keywords:

Density functional theory  
Becke-Johnson model  
Molecular dynamics  
Surface wetting

## ABSTRACT

Silica has been used in a vast number of micro/nano-fluidic technologies where interactions of water with silica at the molecular level play a key role. In such small systems, an understanding of mass and heat transport or surface wetting relies on accurate calculations of the water-silica interface coupling through atomic interactions. Molecular dynamics (MD) is a convenient tool for such use, but force field parameters for nonbonded interactions are required as an input, which are very limited in literature. These interaction parameters can be predicted by density functional theory, but dispersion forces are not calculated in standard models for electron correlations that additional correction models have been proposed at different levels of sophistications, and still under development. Accordingly, this work employs state of the art quantum chemistry to compute the binding energies. Force field parameters for silica/water van der Waals interactions were calculated, and later tested in MD simulations of water droplet on silica surface. While the standard dispersion corrections overestimated the binding energy, Becke-Johnson model yielded interactions parameters recovering experimentally measured wetting behavior of silica with a water contact angle of approximately 12.4° on the flat and clean silica surface. Results will be useful for the current molecular modelling attempts by providing transferable parameters for simple silica/water van der Waals interactions as an alternative to existing complex surface interaction models.

## 1. Introduction

In recent years, various forms of silica materials have been used in a wide range of nanotechnologies such as DNA analyzers [1], targeted drug delivery [2], biological/chemical agent detectors [3], micro/nano chips [4], atomic force microscopes [5] and nano-membranes [6]. Molecular level interactions between solid domains and liquids define the operation of these applications and a significant amount of effort has been put towards understanding the interface coupling between silica nanostructures and water.

While the experiments are challenging and expensive, molecular dynamics (MD) calculations have been a robust and reliable tool to provide insight to the nano-scale world. However, success of MD simulation is strictly related to the functions that are used to model interatomic potentials. A number of successful force fields have been proposed to model silica. For example, intramolecular interactions between silicon and oxygen atoms can be accurately predicted by using well-validated BKS model of van Beest et al. [7] or by Tersoff potential modified for silica systems by Munetoh et al. [8]. On the other hand, calculating interactions of Silica with other molecules is still

challenging. Recently, complex algorithms such as “Reactive force field for silica” (ReaxFFSiO) proposed by van Duin et al. [9] was further examined by Fogarty et al. [10] and practiced by many [11,12] to resolve surface chemistry of silica. In the majority of current literature, the nonbonded interactions are modeled using the two-body Lennard-Jones (LJ) potential and Coulomb’s law. In such an approach, the required LJ potential parameters between pairs of non-identical molecules are frequently calculated from the parameters of the pair of identical molecules by using simple mixing rules [13]. For instance, the Lorentz–Berthelot (LB) mixing rule utilizes arithmetic mean for molecular diameter and geometric mean for the potential strength. However, the interaction parameters between identical molecules are optimized for a bulk material system, which may need to be re-parameterized for the interaction of nonidentical pairs instead of using mixing rules. For example, MD wetting simulations using LB mixing rule fails to capture wetting behavior of silicon surface since the interaction parameters between oxygen and silicon atoms were overestimated [14]. Multiple authors indicated their concerns and proposed ways to calculate the interaction parameters of non-identical molecules accurately [13–18].

One methodology is the measurement of water contact angle to

\* Corresponding author.

E-mail address: [muratbarisik@iyte.edu.tr](mailto:muratbarisik@iyte.edu.tr) (M. Barisik).

<https://doi.org/10.1016/j.apsusc.2019.144359>

Received 15 July 2019; Received in revised form 7 October 2019; Accepted 9 October 2019

Available online 02 November 2019

0169-4332/ © 2019 Elsevier B.V. All rights reserved.

define the interactions of water with corresponding surface. For example, interaction parameters between oxygen atoms of water and silicon atoms of surface was tuned to recover experimentally measured wetting angle on a clean silicon surface [14]. Such methodology yielded very accurate interface modeling for graphene [19] and silicon [14] surfaces. A similar idea was employed for silica by Cruz-Chu et al. [20]; however, instead of changing the interface interactions parameters, the authors changed the potential depth of silicon-silicon interactions to tune the water and silica interaction parameters calculated from mixing rule. Such perspective still suffers from problems arising from mixing rule; the interaction parameters are not transferable to any other MD simulations of silica/water systems.

Instead, interaction parameters between water and silica can be predicted from first principle calculations. Multiple studies were dedicated to develop the nonbonded interaction parameters for an accurate description of coupling between water and various materials, such as molybdenum disulfide [21], hexagonal boron nitride [22] and graphitic carbon [23]. Parametrization of nonbonded interactions is an up-to-date research and a very recent article about current perspectives can be found in [24]. The most commonly used quantum mechanical approach is the Kohn-Sham density functional theory (DFT) [15,25] which has been well-validated. Although, there are many criticisms about the accuracy of DFT, failures are mostly associated with the “density-functional approximation” [26]. Furthermore, due to exchange-correlation functionals required to model interactions between electrons, standard DFT calculation fails to describe long-range electron interactions developing the dispersion or the van der Waals (vdW) forces [27]. Simply, the standard functionals only calculate short-range local properties and do not consider instantaneous fluctuations in electron density. Therefore, additional corrections are needed to capture vdW forces in DFT calculations. A vast number of studies were dedicated to develop DFT-based dispersion techniques. With an interesting analogy, Klimes and Michaelides tried to classify and rank the existing methods through the “stairway to heaven” from “the most approximate to the more sophisticated” approaches for long range dispersion interactions [27]. The basic step for DFT with dispersion (DFT-D) is to introduce a pairwise additive energy term as  $\sum C_{6-i,j}/r_{6-i,j}^6$  correction, where  $C_{6-i,j}$  denotes the dispersion coefficient, and  $r_{6-i,j}$  is the distance between atom  $i$  and  $j$ . Here,  $C_6$  is assumed to be an elemental property and a constant in the DFT-D1 group. Next, ionization and polarization were coupled for the dispersion coefficient calculations in DFT-D2 methods introduced by Grimme [28]. However, DFT-D1 and DFT-D2 were found inaccurate by many because they employ a constant dispersion coefficient. Both methods also employ the earlier mentioned LB mixing rule for the estimation of dispersion coefficient, which is also problematic. Instead of a predetermined and constant dispersion coefficient, DFT-D3 group were dedicated to considering the environmental dependence of dispersion [29,30]. Among these methods, Becke-Johnson (BJ) model [29,31,32] is the most complicated one. In this method, dispersion coefficients are specified depending on atom polarizability and dipole moments. Although computational cost of BJ method is higher than others, it is presented that coefficients calculated by BJ model is quite accurate.

This study performs DFT calculations between a semi-infinite silica surface and a water molecule to estimate the dispersion forces as a function of their separation distance. We will also calculate potential field by pair-wise Lennard-Jones (L-J) potential between the water molecules and all atoms of the silica. By matching results of DFT and L-J, we will determine the interaction parameters for silica and water. We will test developed parameters as part of an MD study where we will calculate the wetting angle and compare it with experimental findings.

**Table 1**

The interlayer distance ( $t$ ) of bilayer graphene and the lattice parameter ( $a$ ) of bulk silicon crystal calculated with different vdW corrections in comparison with the experimental results.

	$t$ (Å)	$a$ (Å)
Experimental	3.40 [39]	5.416 [40,41]
LDA	3.29	5.403
GGA		5.468
GGA-D2	3.26	5.412
GGA-D3 (Zero Damping)	3.44	5.412
GGA-D3 (Becke Jonson Damping)	3.40	5.420
GGA-TS	3.36	5.446
GGA-MBD@rsSCS	4.17	5.468
GGA-DDsC	4.03	5.468

## 2. Methodology

### 2.1. Details of DFT calculations

To investigate the interactions between silica surface and water molecule; first principle calculations were performed using the projector augmented wave (PAW) method [33,34] implemented in the Vienna ab-initio simulation package (VASP). Exchange correlation potentials of the structure were defined with the Perdew-Burke-Ernzerhof (PBE) model of Generalized Gradient Approximation (GGA) functional [35]. Earlier versions for electron correlation with dispersion forces were found overestimating the binding energies [22,36,37]. Specifically, DFT-D2 following Grimme’s method [28] and PBE-TS following the methods of Tkatchenko and Scheffler [30] yielded high interaction parameters which underestimated the water wetting angles. Through the several tests we performed, DFT-D3 method with Becke-Jonson damping [38] gave consistent results with the experimental ones. For example, we calculated the interlayer distance ( $t$ ) of bilayer graphene and the lattice parameter ( $a$ ) of bulk silicon crystal using different dispersion correction models and compared them with corresponding experimental measurements as presented in Table 1. The GGA-D3 with Becke Jonson Damping yielded results closest to experimental values.

Similarly, the GGA-D3 with Becke Jonson calculated 4.919 Å lattice constant for  $\alpha$ -quartz silica, which is almost identical to experimentally measured constant as 4.916 Å [42]. Therefore, DFT-D3 method with Becke-Jonson damping was used as the correction onto GGA for the identification of electron-electron correlation in order to get more accurate vdW interactions between H<sub>2</sub>O and silica surface. The cut-off kinetic energy for each plane wave basis was kept limited to 500 eV and the total energy difference among two electronic steps was specified as  $10^{-5}$  eV as the convergence criterion. Gaussian smearing method was used to obtain partial occupancies with a width of 0.05 eV. Optimization calculations of single silica and water structures were performed until the pressure falls below 1 kbar along the x, y and z directions. To generate (1 0 0) surface of silica and to avoid interactions between adjacent slabs, a 35 Å height vacuum space was created along the x axis. A conventional cell of silica with lattice parameter of  $a = 9.83$  Å and  $b = 10.70$  Å was used to avoid possible interaction of water with itself through the periodic boundary conditions. For construction of the truncated silica surface slab, dangling bonds at the lowermost layer were terminated by H atoms. The 8 Å thick slab was found adequate to mimic the 3D bulk structure.

### 2.2. Details of MD calculations

MD simulation of a water nanodroplet on silica surface was performed to test the interaction parameters determined from DFT. Simulation was 4 nm  $\times$  16 nm  $\times$  10 nm size in x  $\times$  y  $\times$  z-directions. Periodicity condition was applied at x and y directions. A reflecting wall boundary condition was applied 8 nm above silica surface which flips the velocity of water molecules and returns them back to simulation

**Table 2**  
Molecular interaction parameters used for SPC/E water model.

Molecule Pair	$\sigma$ (Å)	$\epsilon$ (eV)	q (e)
O–O	3.166	0.006739	−0.8476
H–H	0	0	0.4238
Si–O [14]	2.633	0.01511	0

domain. The molecules at the lowest layer of silica slab were fixed to their original position to keep the volume constant. Tersoff style silica potential [8] was employed to model  $\alpha$ -quartz structure. LAMMPS (Large-scale Atomic/Molecular Massively Parallel Simulator) Code [43] was used as the MD solver. A hemi-cylindrical droplet was formed with 1280 water molecules. SPC/E model was chosen as the water model due to simplicity and computational cost. Accordingly, length of OH bond and H-O-H angle was constrained with SHAKE algorithm as 0.1 nm and 109.47°, respectively. Oxygen and hydrogen atoms of water are charged with 0.4238e and −0.8476e, respectively. A 1 nm cut off distance was defined for both dispersive and Coulombic interactions between water molecules while particle-particle particle-mesh (PPPM) solver is used to evaluate long-range Coulombic forces among water molecules. Dispersive interactions are modeled with L-J potential given as,

$$\Phi(r_{ij}) = 4\epsilon \left( \left( \frac{\sigma}{r_{ij}} \right)^{12} - \left( \frac{\sigma}{r_{ij}} \right)^6 \right) \quad (1)$$

where  $r_{ij}$  is the intermolecular distance,  $\epsilon$  is the depth of the potential well,  $\sigma$  is the molecular diameter. The interaction parameters for similar molecular pairs used in the simulations are given in Table 2. Interaction parameters between similar materials were taken from the corresponding model. For example, interaction parameters between silica atoms were defined by the Tersoff model while interactions between water molecules were from SPC/E model. On the other hand, for the interaction parameters between dissimilar molecules, it is a common practice through MD studies to estimate these parameters using various forms of mixing rules. For example, for the silicone-oxygen interactions, parameters can be calculated by the LB mixing rule given as,

$$\sigma_{Si-O} = \frac{\sigma_{Si-Si} + \sigma_{O-O}}{2}, \quad \epsilon_{Si-O} = \sqrt{\epsilon_{Si-Si} \times \epsilon_{O-O}} \quad (2)$$

Using the corresponding parameters given in Table 2, the L-B mixing rule predicts the interaction parameters  $\sigma_{Si-O} = 2.6305$  Å and  $\epsilon_{Si-O} = 0.12088$  eV. However, our earlier wetting study based on MD measured contact angles of water nanodroplets showed that interaction parameters from LB do not create the wetting behavior of a clean silicon

surface. Instead, the experimentally measured hydrophobic behavior of silicon surfaces can be recovered when the silicon-oxygen interaction strength is 12.5% of the value predicted by the LB mixing rule [14]. For such a case, we employed this previously proposed interaction strength value for the interaction between  $Si_{Silica}$  and  $O_{Water}$  as  $\epsilon_{Si-O} = 0.01511$  eV, while the interaction parameters for  $O_{Silica}$ - $O_{Water}$  were determined from DFT calculations.

The Verlet algorithm was applied to integrate Newton's equation of motion with a time step of 0.001 ps. At the beginning of simulations, Maxwell-Boltzmann velocity distribution was assigned for all molecules at 300 K. Nose Hoover style NVT ensemble was applied to keep the temperature at 300 K. Simulations are carried out  $2 \times 10^6$  timesteps (2 ns) to reach an isothermal steady state. After that, microcanonical ensemble was employed to obtain averaging of the desired properties for  $6 \times 10^6$  timesteps (6 ns). Averaging is performed with 5 ps intervals. Two different binning were used for averaging. Due to the hemi-cylindrical droplet shape, long rectangular prisms with the size of 0.1 nm  $\times$  infinity  $\times$  0.1 nm along x, y, and z directions were used to resolve droplets. On the other hand, slab bins with infinity  $\times$  infinity  $\times$  0.01 nm along x, y, and z directions were used to resolve silicon domain.

### 3. Results and discussions

The ab initio total energy optimization calculations were performed to estimate the total interaction energies between a water molecule and silica (1 0 0) surface of alpha quartz, to develop force field parameters for LJ potential model. First, we investigated how the single water molecule was adsorbed on the different sites of the silica surface. In order to find the possible adsorption sites, the water molecules were located at various points on silica (1 0 0) surface and geometric optimizations were performed for each.

Possible adsorption sites are represented in Fig. 1(a). While the molecule that was located on the uppermost silicon atom retained its position (site-1), molecules located above the center of the valley and between the closest topmost silicon atoms slightly shifted their initial points (site-2 and site-3). Even though site-2 and site-3 are similar in position, depending on the orientation of the water molecule, site-2 and site-3 differentiated. Site-2 and site-3 developed much higher binding energies than site-1; so that site-1 is more suitable to represent non-bonded interactions. Consequently, the approaching water molecules firstly terminated the lattice points around site-2 and site-3 which resulted in strong binding energies. After the saturation of these highly interactive sites, water molecules settled onto points similar to site-1. As an arbitrary chosen adsorption site, site-4 was also taken into

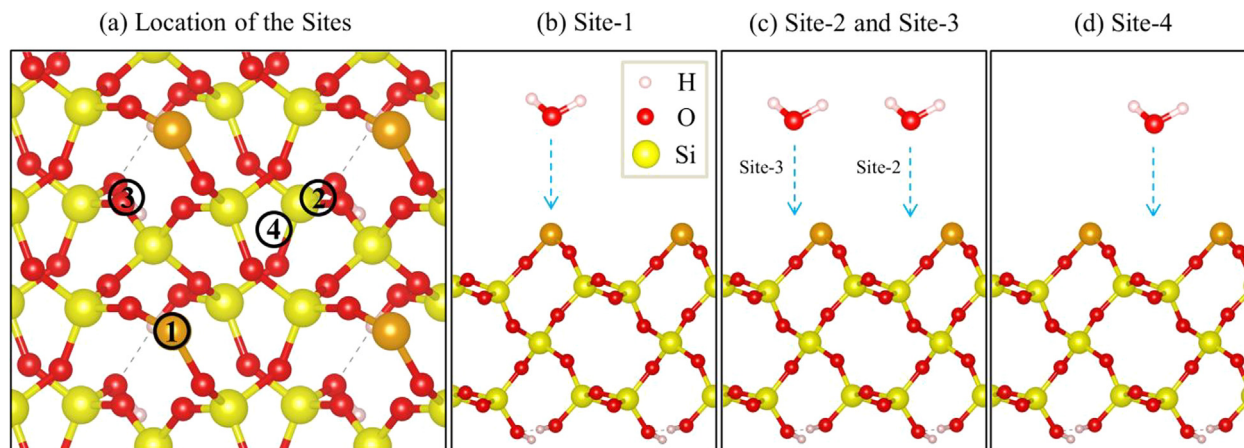


**Fig. 1.** (a) Top view of silica (1 0 0) surface and the adsorption sites for water molecules after structural optimizations. (b)–(d) are side views of site-1, site-2 and site-3, and site-4, respectively. Orange colored atoms represent the topmost silicon atoms. (For interpretation of the references to colour in this figure legend, the reader is referred to the web version of this article.)

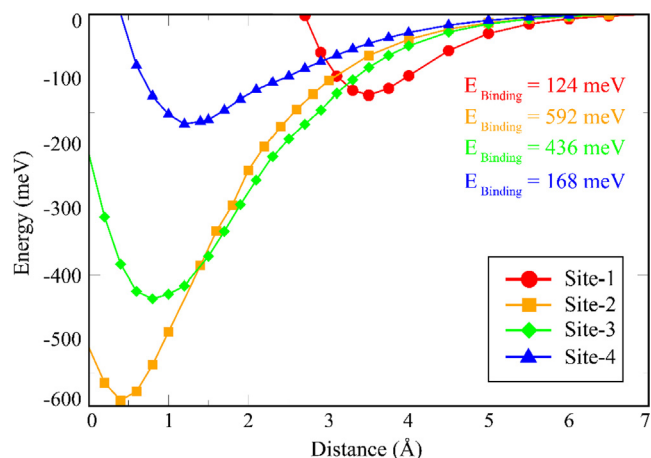


**Fig. 2.** Energy vs distance curves of different sites on alpha quartz (100) surface and binding energies of the sites.

**Table 3**

Molecular interaction parameters fitted for O-O<sub>w</sub> water model.

	Site 1	Site 2	Site 3	Site 4
$\epsilon_{O_{Si}-O_w}$	0.012	0.075	0.38	0.028

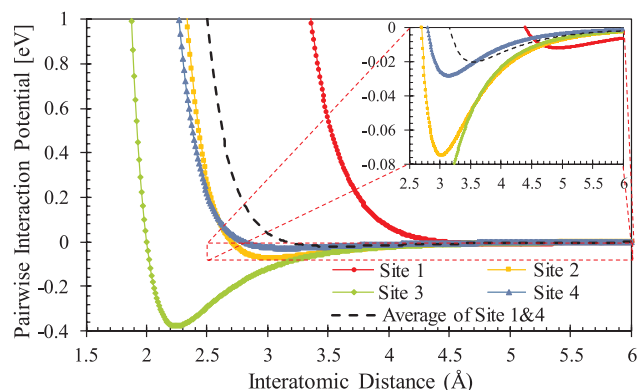


**Fig. 3.** Potential energy between oxygen of water and oxygen atoms of silica as a function of separation distance.

account to describe the behavior of water molecules on weakly interacted points. Here, indentation process was performed on each site to find the exact binding energies between water molecule and silica surface.

Before starting the indentation process, a water molecule was placed above from the topmost silicon atom at least 7 Å and moved to the surface step by step in a controlled manner to obtain the exact potential energy curves of each site. In each step of indentation, oxygen of water molecule was fixed, while hydrogen atoms were free to move

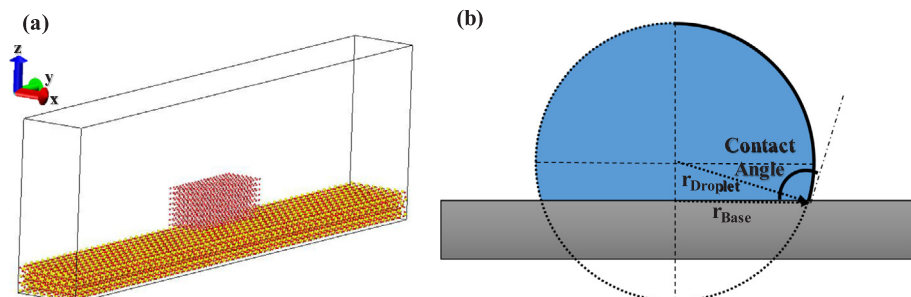


**Fig. 4.** (a) Snapshot of domain at the beginning of molecular dynamics simulation. Silicon, oxygen and hydrogen atoms presented in yellow, red and white, respectively. (b) Schematic illustration of water droplet and its contact angle. (For interpretation of the references to colour in this figure legend, the reader is referred to the web version of this article.)

with respect to the position of oxygen atom to find their most favorable adsorption configuration at each step. It was seen that upon indentation, binding energies varied on each site. The interaction potential profile of site 2 and site-3 showed comparably strong interaction at the silica-water interface (Fig. 2). Their energies were calculated to be 592 meV and 436 meV. Besides, lower binding energies were observed from site 1 and site 4. Their binding energies were 124 meV (site 1) and 0.168 meV (site 4).

Next, interaction energy between water molecule and silica surface was extracted by subtracting energies of water molecule and silica structure from total energy of systems. Fundamentally, current water and silica system interacted through dispersive forces and these vdW forces developed due to the interactions of oxygen of water with the silicon and oxygen atoms of silica. Through such perspective, we hypothesized that obtained potential energy curves are in the form of L-J function as,

$$\Delta E = \sum_i 4\epsilon_{Si-O_w} \left( \left( \frac{\sigma_{Si-O_w}}{r_{Si-O_w}} \right)^{12} - \left( \frac{\sigma_{Si-O_w}}{r_{Si-O_w}} \right)^6 \right) + \sum_i 4\epsilon_{O_{Si}-O_w} \left( \left( \frac{\sigma_{O_{Si}-O_w}}{r_{O_{Si}-O_w}} \right)^{12} - \left( \frac{\sigma_{O_{Si}-O_w}}{r_{O_{Si}-O_w}} \right)^6 \right) \quad (3)$$

where subscripts Si, O<sub>Si</sub> and O<sub>w</sub> denote silicon atoms in silica, oxygen atoms in silica and oxygen atom of the water molecule, respectively. The first term on the right-hand side calculates interactions between the oxygen of water with every Si atom in silica while the second term of right side calculates interactions between the oxygen of water with every oxygen of silica. Eq. (3) requires four parameters, interaction strengths and diameters. The well-known practice is to estimate interaction diameters as the mean of vdW diameters of corresponding atoms. However, using a mixing rule to determine interaction strength between dissimilar atoms creates inaccurate interface coupling, as we described in earlier sections. Alternatively, we employed interaction strength between silicon and oxygen of water from our earlier study [14] and estimate interaction strength between oxygen of silica and oxygen of water from DFT results presented in Fig. 2. For such a case, pairwise interaction of dissimilar oxygen atoms was extracted from total energies for every site. For every site of silica surface, we applied L-J potential calculations between water and silica defined by Eq. (3) as a curve fit onto the potential energy curves from DFT calculations. Resulting interaction strength parameters between oxygen of water and oxygen of silica are given in Table 3. Interaction energies calculated from these interaction strengths are given in Fig. 3. Very high binding energies were measured at site 2 and 3 is due to tendency for bond formation. At these sites, interaction strength values were measured very high; maximum interaction strength was extracted from site 3 although maximum binding energy is obtained from site 2. Since binding energy depends on local electron density but, due to additive pairwise potentials, interaction strength is affected by orientation of atoms and distance between pairs. Thus, site that have maximum binding energy and site that maximum interaction strength could

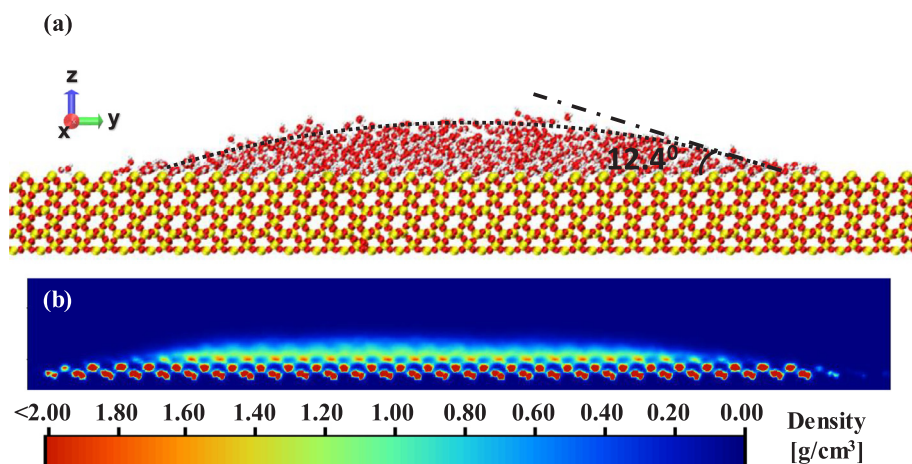


Fig. 5. (a) Representative measurement of contact angle from hemispherical droplet. Silicon, oxygen and hydrogen atoms presented in yellow, red and white, respectively. (b) Average of density distribution of water molecules. (For interpretation of the references to colour in this figure legend, the reader is referred to the web version of this article.)

mismatch. On the other hand, sites with moderate binding energies showed a correct estimation for the corresponding non-bonded interactions. We observed that strengths calculated from these sites, site 1 and 4, represent the parameters of L-J interactions. Therefore, we averaged behavior corresponding to non-bonded interactions from DFT by simply calculating the average of parameters on site 1 and 4 as the vdW interaction strength between oxygen atoms of water and silica.

Next, we employed this interaction parameter in the MD simulation of a water droplet on silica surface. Our objective here was to study wetting behavior and compare it with experimental measurements. At nano-scales, line tension becomes a dominant mechanism proportional with the reciprocal of the contact line radius as a curvature effect at the contact line. In order to eliminate size dependent line tension effects, we formed our water droplet in a semi cylindrical shape to assure a scale effect free contact angle measurement. Fig. 4(a) presents simulation domain at time zero. Size of solid slab in  $-y$  direction was kept long enough to prevent interaction of water molecules through periodic boundaries. Contact angle measurement is described in Fig. 4(b).

Fig. 5(a) presents equilibrium system with the contact angle measurement on it. The averaged density contour is also given in Fig. 5(b). A circular segment is fitted onto density contours. Then the contact angle was calculated from the measured base radius and droplet radius values. Water showed high wetting on silica surface. Wetting angle of approximately  $12.4^\circ$  was measured. There is a strong water layering on silica representing high physisorption.

Although, experimental studies on wetting of alpha quartz silica present a wide range of contact angles from  $7^\circ$  to  $92^\circ$ , it was validated that such inconsistencies are due to surface contaminations. Wetting angle on alpha quartz surface with appropriate surface cleaning procedures were found in between  $0^\circ$  and  $30^\circ$  [44]. Furthermore, recent studies showed that such variation ( $0\text{--}30^\circ$ ) is due to aging and ionic species in water droplets. It was found that contact angle of clean and non-aged quartz surface with deionized water remain around  $10^\circ$  [45]. Therefore, our MD result is in a good agreement with experimental studies, such that the current silica-water non-bonded interaction parameters can successfully reproduce wetting properties of clean, non-aged alpha quartz surface.

#### 4. Conclusion

Binding energy between a silica slab and a water molecule was calculated using density functional theory (DFT), in order to provide nonbonded molecular interactions parameters for Molecular Dynamics (MD) simulations. In the current literature, required parameters for the interaction of dissimilar atoms are frequently estimated using mixing models from the interaction parameters of identical pairs. However, such approach yields interface coupling different than the

experimentally measured behavior. Instead, required interaction parameters can be predicted by DFT. But, in the standard DFT calculations, dispersion forces are not considered in electron correlations so that additional correction models are required. These dispersion correction models are still under development and there are multiple models at different levels of sophistications in literature. We tested different dispersion correction models to calculate structural parameters of bilayer graphene, silicon and silica. The Becke-Johnson model for long-range electron interactions yielded results closest to experimental measurements. Using DFT-D3 method with Becke-Johnson damping, binding energies at different sites were estimated by performing indentation of water molecule onto silica slab. We determined the binding sites developing pure nonbonded interactions, using which interaction parameters between oxygen atoms of silica and water were calculated from potential energy curves. Using the estimated parameters for silica/water van der Waals interactions, we performed molecular dynamics simulations of water droplet on silica surface. Observed surface wetting recovered experimentally measured wetting behavior of silica with a water contact angle of approximately  $12.4^\circ$  on the flat and clean silica surface. Providing proper interaction parameters for the Lennard Jones model is an accurate and also simple alternative to existing complex surface interaction models.

#### Declaration of Competing Interest

The authors declare that they have no known competing financial interests or personal relationships that could have appeared to influence the work reported in this paper.

#### Acknowledgements

This work was supported by the Scientific and Technological Research Council of Turkey (TÜBİTAK) under the Grant Number 217M460. Authors would like to thank Center for Scientific Computation at Southern Methodist University. Dr. Barisik also thanks for the support from the Turkish Academy of Sciences (TUBA) in the framework of the Young Scientist Award Programme (GEBIP).

#### References

- [1] S.K. Min, W.Y. Kim, Y. Cho, K.S. Kim, Fast DNA sequencing with a graphene-based nanochannel device, *Nat. Nanotechnol.* (2011), <https://doi.org/10.1038/nnano.2010.283>.
- [2] M. Vallet-Regí, M. Colilla, I. Izquierdo-Barba, M. Manzano, Mesoporous silica nanoparticles for drug delivery: current insights, *Molecules* (2018), <https://doi.org/10.3390/molecules23010047>.
- [3] M. Kaasalainen, E. Mäkilä, J. Riikonen, M. Kovalainen, K. Järvinen, K.H. Herzig, V.P. Lehto, J. Salonen, Effect of isotonic solutions and peptide adsorption on zeta potential of porous silicon nanoparticle drug delivery formulations, *Int. J. Pharm.* (2012), <https://doi.org/10.1016/j.ijpharm.2012.04.059>.

- [4] X. Chen, L. Zhang, Review in manufacturing methods of nanochannels of bio-nanofluidic chips, *Sens. Actuators B Chem.* (2018), <https://doi.org/10.1016/j.snb.2017.07.139>.
- [5] L. Chu, A.V. Korobko, A. Cao, S. Sachdeva, Z. Liu, L.C.P.M. de Smet, E.J.R. Sudhölter, S.J. Picken, N.A.M. Besseling, Mimicking an atomically thin “Vacuum Spacer” to measure the Hamaker constant between graphene oxide and silica, *Adv. Mater. Interfaces* (2017), <https://doi.org/10.1002/admi.201600495>.
- [6] Y.P. Ying, S.K. Kamarudin, M.S. Masdar, Silica-related membranes in fuel cell applications: an overview, *Int. J. Hydrogen Energy.* (2018), <https://doi.org/10.1016/j.ijhydene.2018.06.171>.
- [7] B.W.H. Van Beest, G.J. Kramer, R.A. Van Santen, Force fields for silicas and aluminophosphates based on ab initio calculations, *Phys. Rev. Lett.* 64 (1990) 1955–1958, <https://doi.org/10.1103/PhysRevLett.64.1955>.
- [8] S. Munetoh, T. Motooka, K. Moriguchi, A. Shintani, Interatomic potential for Si-O systems using Tersoff parameterization, *Comput. Mater. Sci.* 39 (2007) 334–339, <https://doi.org/10.1016/j.commatsci.2006.06.010>.
- [9] A.C.T. Van Duin, A. Strachan, S. Stewman, Q. Zhang, X. Xu, W.A. Goddard, ReaxFFSiO reactive force field for silicon and silicon oxide systems, *J. Phys. Chem. A.* 107 (2003) 3803–3811, <https://doi.org/10.1021/jp0276303>.
- [10] J.C. Fogarty, H.M. Aktulga, A.Y. Grama, A.C.T. Van Duin, S.A. Pandit, A reactive molecular dynamics simulation of the silica-water interface, *J. Chem. Phys.* 132 (2010), <https://doi.org/10.1063/1.3407433>.
- [11] J.M. Rimsza, J. Yeon, A.C.T. Van Duin, J. Du, Water interactions with nanoporous silica: comparison of ReaxFF and ab initio based molecular dynamics simulations, *J. Phys. Chem. C* (2016), <https://doi.org/10.1021/acs.jpcc.6b07939>.
- [12] Y. Yu, N.M.A. Krishnan, M.M. Smedskjaer, G. Sant, M. Bauchy, The hydrophilic-to-hydrophobic transition in glassy silica is driven by the atomic topology of its surface, *J. Chem. Phys.* (2018), <https://doi.org/10.1063/1.5010934>.
- [13] A.K. Al-Matar, D.A. Rockstraw, A generating equation for mixing rules and two new mixing rules for interatomic potential energy parameters, *J. Comput. Chem.* (2004), <https://doi.org/10.1002/jcc.10418>.
- [14] M. Barisik, A. Beskok, Wetting characterisation of silicon (1 0 0) surface, *Mol. Simul.* 39 (2013) 700–709, <https://doi.org/10.1080/08927022.2012.758854>.
- [15] W. Kohn, L.J. Sham, Self-consistent equations including exchange and correlation effects, *Phys. Rev.* 140 (1965) A1133, <https://doi.org/10.1103/PhysRev.140.A1133>.
- [16] B. Ramos-Alvarado, S. Kumar, G.P. Peterson, Wettability of graphitic-carbon and silicon surfaces: MD modeling and theoretical analysis, *J. Chem. Phys.* 143 (2015), <https://doi.org/10.1063/1.4927083>.
- [17] C.U. Gonzalez-Valle, S. Kumar, B. Ramos-Alvarado, Investigation on the wetting behavior of 3C-SiC surfaces: theory and modeling, *J. Phys. Chem. C* (2018), <https://doi.org/10.1021/acs.jpcc.7b12271>.
- [18] M. Fyta, R.R. Netz, Ionic force field optimization based on single-ion and ion-pair solvation properties: going beyond standard mixing rules, *J. Chem. Phys.* (2012), <https://doi.org/10.1063/1.3693330>.
- [19] T. Werder, J.H. Walther, R.L. Jaffe, T. Halicioglu, P. Koumoutsakos, On the water-carbon interaction for use in molecular dynamics simulations of graphite and carbon nanotubes, *J. Phys. Chem. B.* 107 (2003) 1345–1352, <https://doi.org/10.1021/jp0268112>.
- [20] E.R. Cruz-Chu, A. Aksimentiev, K. Schulten, Water-silica force field for simulating nanodevices, *J. Phys. Chem. B* 110 (2006) 21497–21508, <https://doi.org/10.1021/jp063896o>.
- [21] M. Heiraniyan, Y. Wu, N.R. Aluru, Molybdenum disulfide and water interaction parameters, *J. Chem. Phys.* 147 (2017), <https://doi.org/10.1063/1.5001264>.
- [22] Y. Wu, L.K. Wagner, N.R. Aluru, Hexagonal boron nitride and water interaction parameters, *J. Chem. Phys.* 144 (2016), <https://doi.org/10.1063/1.4947094>.
- [23] Y. Wu, N.R. Aluru, Graphitic carbon-water nonbonded interaction parameters, *J. Phys. Chem. B* (2013), <https://doi.org/10.1021/jp402051t>.
- [24] Y.S. Al-Hamdani, A. Tkatchenko, Understanding non-covalent interactions in larger molecular complexes from first principles, *J. Chem. Phys.* (2019), <https://doi.org/10.1063/1.5075487>.
- [25] P. Hohenberg, W. Kohn, Inhomogeneous electron gas, *Phys. Rev.* 136 (1964) B864, <https://doi.org/10.1103/PhysRev.136.B864>.
- [26] A.D. Becke, Perspective: Fifty years of density-functional theory in chemical physics, *J. Chem. Phys.* (2014), <https://doi.org/10.1063/1.4869598>.
- [27] J. Klimeš, A. Michaelides, Perspective: advances and challenges in treating van der Waals dispersion forces in density functional theory, *J. Chem. Phys.* (2012), <https://doi.org/10.1063/1.4754130>.
- [28] S. Grimme, Semiempirical GGA-type density functional constructed with a long-range dispersion correction, *J. Comput. Chem.* (2006), <https://doi.org/10.1002/jcc.20495>.
- [29] A.D. Becke, Real-space post-Hartree-Fock correlation models, *J. Chem. Phys.* (2005), <https://doi.org/10.1063/1.1844493>.
- [30] A. Tkatchenko, M. Scheffler, Accurate molecular van der Waals interactions from ground-state electron density and free-atom reference data, *Phys. Rev. Lett.* (2009), <https://doi.org/10.1103/PhysRevLett.102.073005>.
- [31] A.D. Becke, E.R. Johnson, A density-functional model of the dispersion interaction, *J. Chem. Phys.* (2005), <https://doi.org/10.1063/1.2065267>.
- [32] E.R. Johnson, A.D. Becke, A post-Hartree-Fock model of intermolecular interactions: Inclusion of higher-order corrections, *J. Chem. Phys.* (2006), <https://doi.org/10.1063/1.2190220>.
- [33] G. Kresse, J. Hafner, *Ab initio* molecular dynamics for liquid metals, *Phys. Rev. B* 47 (1993) 558–561, <https://doi.org/10.1103/PhysRevB.47.558>.
- [34] G. Kresse, J. Furthmüller, Efficient iterative schemes for *ab initio* total-energy calculations using a plane-wave basis set, *Phys. Rev. B* 54 (1996) 11169–11186, <https://doi.org/10.1103/PhysRevB.54.11169>.
- [35] J.P. Perdew, K. Burke, M. Ernzerhof, Generalized gradient approximation made simple, *Phys. Rev. Lett.* 77 (1996) 3865–3868, <https://doi.org/10.1103/PhysRevLett.77.3865>.
- [36] Y. Wu, L.K. Wagner, N.R. Aluru, The interaction between hexagonal boron nitride and water from first principles, *J. Chem. Phys.* (2015), <https://doi.org/10.1063/1.4922491>.
- [37] T.A. Hilder, R. Yang, V. Ganesh, D. Gordon, A. Bliznyuk, A.P. Rendell, S.-H. Chung, Validity of current force fields for simulations on boron nitride nanotubes, *Micro Nano Lett.* (2010), <https://doi.org/10.1049/mnl.2009.0112>.
- [38] S. Grimme, S. Ehrlich, L. Goerigk, Effect of the damping function in dispersion corrected density functional theory, *J. Comput. Chem.* 32 (2011) 1456–1465, <https://doi.org/10.1002/jcc.21759>.
- [39] T. Ohta, A. Bostwick, T. Seyller, K. Horn, E. Rotenberg, Controlling the electronic structure of bilayer graphene, *Science* 313 (5789) (2006) 951–954, <https://doi.org/10.1126/science.1130681>.
- [40] G.I. Csonka, J.P. Perdew, A. Ruzsinszky, P.H.T. Philipsen, S. Lebègue, J. Paier, O.A. Vydrov, J.G. Ángyán, Assessing the performance of recent density functionals for bulk solids, *Phys. Rev. B – Condens. Matter Mater. Phys.* (2009), <https://doi.org/10.1103/PhysRevB.79.155107>.
- [41] N. Data, Functional relationships in science and technology, in: K.-H. Hellwege, A.M. Hellwege (Eds.), *Landolt–Börnstein, New Series, Gr. III. 11* 1982.
- [42] N.R. Keskar, J.R. Chelikowsky, Structural properties of nine silica polymorphs, *Phys. Rev. B* (1992), <https://doi.org/10.1103/PhysRevB.46.1>.
- [43] S. Plimpton, Fast parallel algorithms for short-range molecular dynamics, *J. Comput. Phys.* 117 (1995) 1–19, <https://doi.org/10.1006/jcph.1995.1039>.
- [44] S. Iglauer, A. Salamah, M. Sarmadivaleh, K. Liu, C. Phan, Contamination of silica surfaces: Impact on water-CO<sub>2</sub>-quartz and glass contact angle measurements, *Int. J. Greenh. Gas Control.* 22 (2014) 325–328, <https://doi.org/10.1016/j.ijggc.2014.01.006>.
- [45] Z. Qi, Y. Wang, H. He, D. Li, X. Xu, Wettability alteration of the quartz surface in the presence of metal cations, *Energy Fuels* 27 (2013) 7354–7359, <https://doi.org/10.1021/ef401928c>.